Characterization of the Heme in Human Cystathionine β-Synthase by X-ray Absorption and Electron Paramagnetic Resonance Spectroscopies†

Sunil Ojha,‡ Jungwon Hwang,§ Ömer Kabil,‡ James E. Penner-Hahn,*,§ and Ruma Banerjee*,‡

Department of Chemistry, University of Michigan, Ann Arbor, Michigan 48109-1055, and Department of Biochemistry, University of Nebraska, Lincoln, Nebraska 68588-0664

Received April 12, 2000; Revised Manuscript Received June 15, 2000

ABSTRACT: Human cystathionine β-synthase is one of two key enzymes involved in intracellular metabolism of homocysteine. It catalyzes a β-replacement reaction in which the thiolate of homocysteine replaces the hydroxyl group of serine to give the product, cystathionine. The enzyme is unusual in its dependence on two cofactors: pyridoxal phosphate and heme. The requirement for pyridoxal phosphate is expected on the basis of the nature of the condensation reaction that is catalyzed; however the function of the heme in this protein is unknown. We have examined the spectroscopic properties of the heme in order to assign the axial ligands provided by the protein. The heme Soret peak of ferric cystathionine β-synthase is at 428 nm and shifts to ~395 nm upon addition of the thiol chelator, mercuric chloride. This is indicative of 6-coordinate low-spin heme converting to a 5-coordinate high-spin heme. The enzyme as isolated exhibits a rhombic EPR signal with g values of 2.5, 2.3, and 1.86, which are similar to those of heme proteins and model complexes with imidazole/thiolate ligands. Mercuric chloride treatment of the enzyme results in conversion of the rhombic EPR signal to a $g = 6$ signal, consistent with formation of the high-spin ferric heme. The X-ray absorption data reveal that iron in ferric cystathionine β-synthase is 6-coordinate, with 1 high-Z scatterer and 5 low-Z scatterers. This is consistent with the presence of 5 nitrogens and 1 sulfur ligand. Together, these data support assignment of the axial ligands as cysteinate and imidazole in ferric cystathionine β-synthase.

The transsulfuration reaction catalyzed by cystathionine β-synthase represents one of two major avenues for metabolism of homocysteine in mammals. Elevated levels of homocysteine are correlated with a number of apparently unrelated disease pathologies including atherosclerosis (reviewed in ref *1*), neural tube defects (*2*, *3*), and Alzheimer's disease (*4*, *5*). Mutations in cystathionine β-synthase are the single most common cause of homocystinuria, an inborn error of metabolism that is inherited as an autosomal recessive disease (*6*, *7*). Cystathionine β-synthase catalyzes the condensation of serine and homocysteine to generate cystathionine that is subsequently converted to cysteine. This reaction is dependent on pyridoxal phosphate (PLP)[1] and appears to be mechanistically related to other B_6-dependent enzymes that catalyze β-replacement reactions such as tryptophan synthase (*8*). The human enzyme contains a second cofactor, iron protoporphyrin IX, whose role in this protein remains enigmatic (*9*). The activity of the enzyme is enhanced ~2-fold under maximal velocity conditions by the allosteric regulator, AdoMet (*10*).

The native enzyme exists as a homotetramer and is composed of 63 kDa monomers. Two hemes and four PLPs are associated with the tetramer (*11*, *12*). Removal of the C-terminal regulatory domain by limited proteolysis of the native enzyme (*13*) or by recombinant methods (*14*) results in the formation of a homodimeric catalytic core composed of ~48 kDa monomers. The truncated enzyme displays high catalytic activity but is unresponsive to AdoMet, consistent with the loss of the putative AdoMet binding site. The truncated enzyme binds one PLP and one heme per monomer, suggesting that tetramerization of the native enzyme is accompanied by a change in heme stoichiometry (*12*, *15*).

At least three alternative roles can be considered for the heme in cystathionine β-synthase, namely, catalytic, regulatory, or structural. While sequence analysis reveals strong homology between cystathionine β-synthase and other PLP enzymes, it appears to be very distantly related to a limited number of heme proteins (*12*). These include cytochrome *c*-550, cytochrome P-450, and sulfide dehydrogenase. On the basis of these sequence comparisons, the N-terminal, middle, and C-terminal regions of cystathionine β-synthase are postulated to be involved in PLP, heme, and AdoMet binding, respectively. The activity of cystathionine β-synthase is redox sensitive and is increased ~2-fold under oxidizing

† This work was supported by grants from the National Institutes of Health (HL58984 to R.B. and GM38047 to J.E.P.-H.). X-ray absorption data were measured at SSRL, which is operated by the DOE, Office of Basic Energy Sciences, with additional support from the NIH, National Center for Research Resources, and the DOE Office of Biological and Environmental Research. R.B. is an Established Investigator of the American Heart Association.

* Corresponding authors. R.B.: tel, (402) 472-2941; fax, (402) 472-7842; e-mail, rbanerjee1@unl.edu. J.E.P.-H.: tel, (734) 764-7324; fax, (734) 647-4865; e-mail, jeph@umich.edu.

‡ University of Nebraska.

§ University of Michigan.

[1] Abbreviations: EXAFS, extended X-ray absorption fine structure; XANES, X-ray absorption near edge structure; EPR, electron paramagnetic resonance; PLP, pyridoxal phosphate; AdoMet, *S*-adenosylmethionine; MCD, magnetic circular dichroism.

10.1021/bi000831h CCC: $19.00
Published on Web 08/03/2000

conditions, which is correlated with the ferric state of the iron (*16*).

The enzyme as isolated contains ferric heme with a Soret absorption peak at 428 nm and a broad α/β absorption band at 550 nm. Reduction of the heme with either dithionite or titanium citrate shifts the Soret peak to 450 nm and sharpens the α and β bands with maxima at 571 and 540 nm, respectively (*16*). The characteristics of the absorption spectra indicate that the iron in both ferric and ferrous heme states is 6-coordinate and low spin. To address the role of the heme in this enzyme, it is essential to understand its properties and, in particular, to identify its axial ligands. In this study, we have employed X-ray absorption and EPR spectroscopies to characterize the ferric heme associated with the enzyme as isolated. These studies provide evidence for imidazole and thiolate coordination to the iron.

MATERIALS AND METHODS

Enzyme Purification. Full-length human cystathionine β-synthase was purified from a recombinant expression system (pGEX4T1/hCBS) described previously (*14*) that produces a fusion protein with glutathione *S*-transferase at the N-terminus. The truncated human CBS lacking 143 amino acids at the C-terminus was also purified as a fusion protein containing glutathione *S*-transferase using the expression vector pGEXCBSN (*14*). Both expression constructs were provided by Warren Kruger (Fox Chase Cancer Center, Philadelphia, PA). The cells were cultured, and the proteins were purified as described previously (*16*). In the last step of purification, the glutathione *S*-transferase domain is cleaved by limited proteolysis using thrombin and purified by chromatography on a DEAE-cellulose column (*16*).

EPR Spectroscopy. EPR spectra were recorded on a Bruker ESP 300E spectrometer equipped with an Oxford ITC4 temperature controller, a Model 5340 automatic frequency counter from Hewlett-Packard, and a gaussmeter. The specific conditions are described in the figure legends. The EPR sample was prepared by concentrating truncated cystathionine β-synthase (to 56 μM in heme) in 100 mM Tris·HCl, pH 8.5. The heme concentration was determined independently by UV−visible absorption spectroscopy using $\epsilon_{428} = 185$ mM^{-1} cm^{-1} (*12*) and by spin quantitation by comparison of the second integral of the sample spectrum with that of a 1 mM cupric perchlorate standard and were comparable.

X-ray Absorption Spectroscopy. Samples were concentrated to 2.2 mM (sample 1) or 3 mM (sample 2) in 50 mM Tris·HCl buffer, pH 8.5, diluted by addition of 30% glycerol to prevent ice formation, and loaded into Lucite cuvettes and quickly frozen in liquid nitrogen. XAS measurements were made at SSRL on beamline 7-3 under dedicated conditions (3.0 GeV, 90−100 mA), using a Si(220) double crystal monochromator detuned to 50% of the maximum intensity for harmonic rejection. Samples were held at 10 K during the measurements using an Oxford helium flow cryostat. Spectra were measured using 10 eV steps in the preedge, 0.25 or 0.30 eV steps in the edge (7100−7140 eV), and 0.05 Å^{-1} steps in the EXAFS region (to $k = 13$ Å^{-1}), integrating for 1 s in the preedge and edge regions, and using k^3-weighted integration times from 1 to 25 s in the EXAFS region, giving a total scan time of ∼45 min/scan. X-ray energies were calibrated by simultaneous measurement of an Fe foil absorption spectrum and assigning the first inflection point of the absorption edge to 7111.2 eV.

X-ray absorption data were collected as fluorescence excitation spectra using a 13-element Ge solid-state detector array, with the incident count rate for each channel held below ∼60 kHz to avoid saturation. The windowed Fe Kα count rates were ∼5 kHz in the EXAFS region, giving a total of ∼10^6 useful counts/scan at $k = 14$ Å^{-1}. The individual channels in each scan were examined for glitches, and all of the good channels (typically 9 per scan) were averaged to give the final spectrum. Two independent samples were studied, one for which 7 scans were measured and one for which 8 scans were measured.

XANES data were normalized by fitting the data below and above the edge to the McMaster X-ray absorption cross sections (*17*), using an error-function background, a second-order polynomial, and a scale factor (Weng, Waldo, and Penner-Hahn, unpublished results). EXAFS background subtraction and data reduction were accomplished by fitting a first-order polynomial through the preedge and a two-region cubic spline through the EXAFS. Data were subsequently converted to *k*-space, where $k = [2m_e(E - E_0)/h^2]^{1/2}$, using $E_0 = 7130$ eV. Fourier transforms of the EXAFS data were calculated using k^3-weighted data from $k = 3.0-12.5$ Å^{-1}. Fits were made to both Fourier-filtered ($R = 0.6-3.1$ Å) and unfiltered data and gave equivalent structural parameters.

EXAFS data are described by eq 1, where $\chi(k)$ is the fractional modulation in the absorption coefficient above the edge, N_s is the number of scatterers, *S*, at a distance R_{as}, $A_s(k)$ is the effective backscattering amplitude, σ^2_{as} is the root-mean-square variation in R_{as}, $\phi_{as}(k)$ is the phase shift experienced by the photoelectron wave in passing through the potentials of the absorbing and backscattering atoms, S_s is a scale factor specific to the absorber−scatterer pair, and the sum is taken over all scattering interactions (*18*). The program FEFF version 6.01 (*19*) was used to calculate the amplitude and phase functions, $A_s(k)$ and $\phi_{as}(k)$, for Fe−N at 2.0 Å, Fe−S at 2.25 Å, and Fe−C at 3.0 and 3.4 Å. No attempt was made to model the Fe−C_β scattering at ∼4.2 Å due to the difficulty of treating the multiple scattering. The scale factor of 0.9 and ΔE_0 of 10.0 eV were calibrated on the basis of fits to ferric porphyrin models.

$$\chi(k) = \sum \frac{N_s A_s(k) S_s}{kR^2_{as}} \exp(-2k^2\sigma^2_{as}) \sin[2kR_{as} + \phi_{as}(k)] \quad (1)$$

RESULTS

Spectral Changes Accompanying $HgCl_2$ Addition. The UV−visible spectrum of cystathionine β-synthase is affected by the thiol-binding reagent, $HgCl_2$ (Figure 1). Addition of $HgCl_2$ results in the slow, time-dependent, conversion of the sharp Soret peak at 428 nm to a broad peak with a maximum at ∼395 nm and isosbestic crossovers at 410, 515, and 599 nm, respectively. The blue shift in the Soret peak is consistent with conversion of a 6-coordinate low-spin ferric heme to a 5-coordinate high-spin ferric heme and strongly suggests that a sulfur ligand is lost on addition of $HgCl_2$. Addition of $HgCl_2$ to dithionite-reduced ferrous enzyme results in a shift in the Soret peak from 450 to 425 nm, indicating loss of

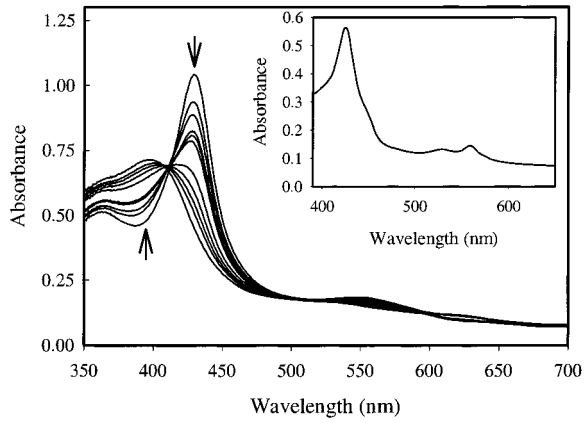

FIGURE 1: Effect of $HgCl_2$ addition on the UV−visible absorption spectrum of ferric cystathionine β-synthase. $HgCl_2$ (0.2 mM) was added to truncated ferric cystathionine β-synthase (12 μM based on heme concentration) in 100 mM Tris·HCl, pH 8.5, and spectra were recorded at 5 min intervals for 1 h. The up and down arrows are at 395 and 428 nm, respectively, and indicate the direction of the time-dependent absorption changes at these wavelengths. Inset: Absorption spectrum of ferrous cystathionine β-synthase. An anaerobic solution of enzyme (6 μM in heme concentration) was treated with $HgCl_2$ (100 μM) and reduced with 100 μM dithionite. The α, β, and Soret bands are at 559, 529, and 425 nm, respectively.

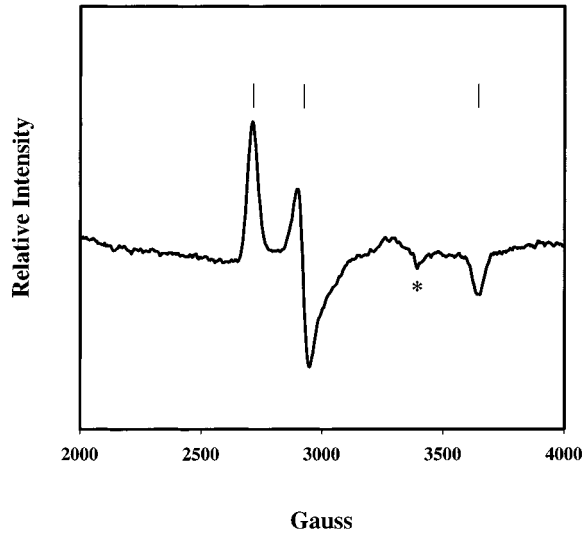

FIGURE 2: X-band EPR spectrum of ferric cystathionine β-synthase. The sample contained enzyme (50.3 μM in heme) in 100 mM Tris·HCl, pH 8.5. The spectrum was recorded at 10 K, 1 mW microwave power, 2×10^4 receiver gain, 12.78 G modulation amplitude, 9.474 GHz microwave frequency, and 100 kHz modulation frequency using 1024 data points. The spectrum represents a single scan. The asterisk denotes a signal present in the cavity. The line markers are at $g = 2.5$, 2.3, and 1.86, respectively.

thiolate ligation but retention of the 6-coordinate state (Figure 1, inset). The identity of the sixth ligand that replaces the thiolate ligand is unknown.

EPR Spectroscopy of Cystathionine β-Synthase. The EPR spectrum of truncated cystathionine β-synthase is rhombic with $g_z = 2.5$, $g_y = 2.3$, and $g_x = 1.86$, characteristic of low-spin heme (Figure 2). These values are similar to those for other heme proteins and model complexes with thiolate and imidazole ligands to the heme (Table 1). The spin concentration of the samples corresponds to the heme concentration estimated from the visible absorption spectra. The EPR spectrum of the enzyme does not change between

Table 1: Comparison of the EPR Spectral Properties of Cystathionine β-Synthase with Model Compounds and Heme Proteins

protein or model	iron ligands	EPR g values	ref
Fe(III) cystathionine β-synthase, pH 8.5		2.5, 2.3, 1.86	this work
Fe(III) PPIX/benzimidazole/mercaptoethanol	BzIm/RS^-	2.48, 2.3, 1.88	*35*
Fe(III) Hb + methanethiol	His/RS^-	2.46, 2.26, 1.9	*36*
Fe(III) Hb + sulfide	His/HS^-	2.47, 2.27, 1.9	*36*
Fe(III) CooA	His/Cys	2.46, 2.26, 1.90	*37*
Fe(III) CooA	His/Cys	2.46, 2.25, 1.89	*38*
Fe(III) P450 + imidazole	imidazole/Cys	2.56, 2.27, 1.87	*39*

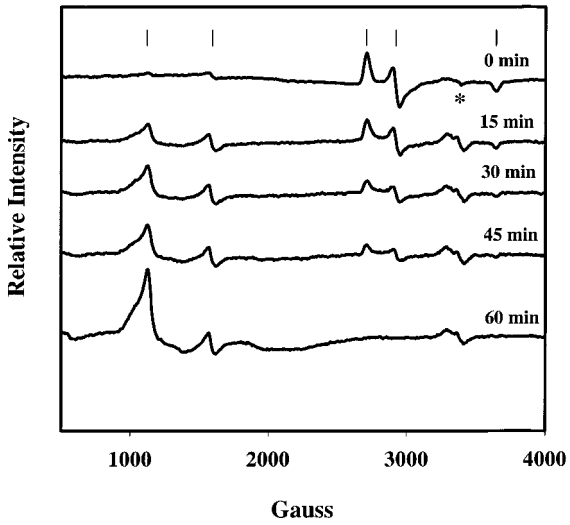

FIGURE 3: Effect of $HgCl_2$ addition on the EPR spectrum of cystathionine β-synthase. The EPR spectra were measured using the same conditions described in Figure 2. The spectrum at 0 min is before $HgCl_2$ treatment. Following addition of 480 μM $HgCl_2$, the sample was allowed to stand at room temperature for 15 min prior to freezing and recording the spectrum. The sample was then thawed and allowed to stand at room temperature for an additional 15 min prior to freezing and spectral recording. This procedure was repeated for the 45 and 60 min time points. The asterisk denotes a signal present in the cavity, and the $g = \sim 4.3$ signal is due to adventitious iron and does not change on addition of $HgCl_2$. The line markers are at $g = 6$, 4, 2.5, 2.3, and 1.86, respectively.

pH 6 and pH 9, indicating that the porphyrin ligands are insensitive to pH, at least over this range. The spectrum of the full-length enzyme is indistinguishable from that of the truncated enzyme (data not shown), indicating that deletion of the regulatory domain does not lead to detectable changes in the heme environment. Addition of $HgCl_2$ to cystathionine β-synthase resulted in a slow, time-dependent, conversion of the low-spin heme to a high-spin species with $g = 6$ (Figure 3).

EXAFS Analysis of Cystathionine β-Synthase. The Fourier transforms of the EXAFS data for two independent samples are shown in Figure 4, together with the XANES data for one of the samples as an inset. The XANES data are consistent with a low-spin iron(III) porphyrin. In particular, the extremely weak 1s → 3d transition indicates a 6-coordinate, pseudo-octahedral Fe geometry (*20*). The Fourier transforms of the EXAFS data show an intense first-shell peak at $R + \alpha \approx 1.7$ Å that is attributable to Fe−N scattering, together with several weaker peaks at higher R. The higher R peaks are characteristic of outer-shell scattering from the rigid porphyrin ring and can be assigned to the $C_\alpha + C_{meso}$

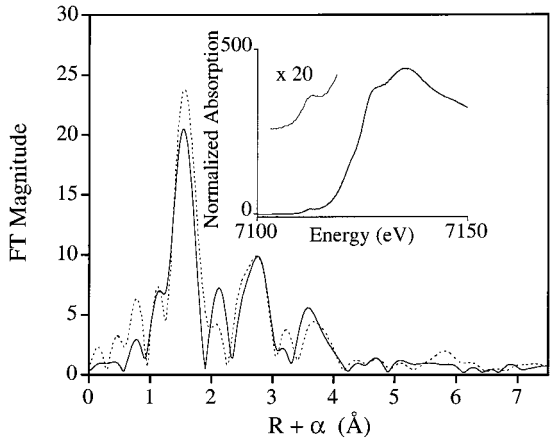

FIGURE 4: Fourier transfer of k^3-weighted EXAFS for cystathionine β-synthase (k = 3−12.5 Å^{-1}): solid line, sample 1; dashed line, sample 2. Inset: XANES spectrum for sample 2. Sample 1 has identical XANES, shifted ~0.1 eV to lower energy. The expansion showing 1s → 3d transition is enlarged 20-fold vertically and 5-fold horizontally.

scattering ($R + \alpha \approx 2.8$ Å) and the C_β scatterers ($R + \alpha \approx 3.6$ Å) (*21*). There is, in addition, a weak fourth peak at $R + \alpha \approx 2.0$ Å. This peak is identical to that seen in the EXAFS data for cytochrome *c*-551 (Stemmler et al., unpublished data) and strongly suggests that there is a heavy scatterer bound to the Fe in cystathionine β-synthase. Although the $R + \alpha \approx 2.0$ Å peak appears to be resolved from the Fe−N and Fe−(C_α + C_{meso}) peaks, it in fact contains contributions from Fe−N, Fe−X (X = high-Z scatterer), and Fe−C scattering (*22*). It is this mixture of contributions that makes the amplitude of the $R + \alpha \approx 2.0$ Å peak extremely sensitive to small variations in average bond length.

The filtered EXAFS corresponding to the nearest-neighbor interactions cannot be well modeled using only a single shell of Fe−N scatterers. However, there is a significant (2-fold) improvement in the fit if a second shell containing a single Fe−S interaction is included. The same result is seen for fits over a wider filter range (large enough to include the C_α and C_{meso} carbons) and for fits to the unfiltered data, although the fractional improvement is smaller (~2-fold) in these cases. No improvement was seen if, instead, two shells of Fe−N scatterers were used to model the nearest-neighbor scattering. The fitting results thus support the qualitative conclusion from the Fourier transforms that there is a heavy scatterer bound to the Fe. EXAFS alone cannot distinguish between Fe−S and Fe−Cl scattering. However, the electronic absorption and EPR spectra strongly suggest that the Fe−X scattering arises from a coordinated cysteine ligand rather than from a chloride. This is confirmed by the observation of identical UV−visible spectra in Cl^--free (potassium phosphate buffer) and Cl^--containing (Tris·HCl) buffers.

The best fits are obtained by assuming a total iron coordination number of 6. Although it is difficult to define coordination number precisely using EXAFS, this structural picture is supported both by the weak 1s → 3d transition and by the refined Fe−N bond length. The observed Fe−N distance of 1.99−2.00 Å is typical of that seen for low-spin 6-coordinate Fe porphyrins and significantly smaller than would be expected if the Fe were 5-coordinate and displaced out of the plane of the porphyrin. The fit quality is equally good for fits assuming 5 Fe−N scatterers and 1 Fe−S scatterer or 4 Fe−N and 2 Fe−S scatterers. However, the fit results (Table 2), strongly argue in favor of the 5 Fe−N/1 Fe−S model. For fits using 5 Fe−N + 1 Fe−S, the Debye−Waller factors for both the Fe−S and the Fe−N shells are typical of those seen in model compounds (*23*). In contrast, fits using 4 Fe−N + 2 Fe−S give Fe−N Debye−Waller factors somewhat smaller than expected and, more importantly, Fe−S Debye−Waller factors more than twice as large as those seen for authentic Fe−S interactions. A nonphysically large Debye−Waller factor is expected if too many scatterers are used in the fit, arguing strongly against the 4 Fe−N/2 Fe−S model. Bond-valence-sum calculations (*24*, *25*) give the expected valence of 3 if the coordination numbers are taken as 5 Fe−N and 1 Fe−S. There is a slight variation between the two samples. This may arise from the presence of a small amount of reduced cystathionine β-synthase in sample 1 (the edge for sample 1 is shifted ~0.1 eV to lower energy relative to the edge for sample 2). This does not affect the structural conclusions.

Table 2: Curve-Fitting Results for Cystathionine β-Synthase[a]

	Fe−N		Fe−S		Fe−C(α)		Fe−C(meso)	
	R^b	$\sigma^{2\,b}$	R^b	$\sigma^{2\,b}$	R^b	$\sigma^{2\,b}$	R^b	$\sigma^{2\,b}$
sample 1								
4 Fe−N/2 Fe−S	1.98	1.1	2.27	9.4	3.03	3.1	3.37	2.4
5 Fe−N/1 Fe−S	1.98	2.0	2.29	3.8	3.04	3.3	3.37	2.1
sample 2								
4 Fe−N/2 Fe−S	2.00	1.0	2.23	8.3	3.03	1.6	3.35	5.5
5 Fe−N/1 Fe−S	2.00	1.3	2.25	2.5	3.03	1.9	3.35	4.7

[a] All fits used 8 Fe−C(α) and 4 Fe−C(meso). [b] R is the absorber−scatterer distance in Å, and σ^2 is the mean square deviation in R in Å^2 × 10^3.

DISCUSSION

Although the properties of cystathionine β-synthase have been studied for a number of years (*26*, *27*), the presence of heme in this protein was realized only recently (*9*), and it remains poorly characterized. The discovery of heme in human cystathionine β-synthase resulted from studies on a rat heme protein, H450. Purification of H450 (*28*) and characterization of the electronic absorption and EPR spectroscopic properties of the heme were reported several years ago (*29*−*31*). Cloning and sequence determination of the gene encoding the rat H450 protein led to the realization that it represented rat cystathionine β-synthase (*32*). The association of heme and PLP with mammalian cystathionine β-synthase is unique in that no other enzyme has been described with a dependence on this combination of cofactors. While the chemistry of the β-replacement reaction catalyzed by cystathionine β-synthase suggests an obvious role for PLP which serves as an electrophilic sink, the role of the heme in this protein is unknown. As a first step toward elucidating the role of the heme in the protein, it is important to characterize the heme environment and to identify the heme ligands. In this study, we have employed EPR and X-ray absorption spectroscopy to assign the ligands to ferric heme in cystathionine β-synthase.

Assignment of the Thiolate Ligand. The UV−visible absorption spectra of ferric and ferrous cystathionine β-synthase are characteristic of low-spin hemes and indicate that

the protein donates two axial ligands (*16*). Some candidate amino acid ligands with ligand field strengths sufficient to generate the low-spin state of heme include histidine, lysine, methionine, and cysteine (*33*). Ferric cystathionine β-synthase has a Soret peak at 428 nm diagnostic of thiolate-ligated, low-spin hemes with a neutral sixth donor ligand (*34*). In addition, the unusually red-shifted Soret peak at 450 nm in the ferrous protein provides strong evidence for the presence of a thiolate ligand. The changes in the spectral properties elicited by addition of the thiol chelator, $HgCl_2$ (Figure 1), are consistent with conversion of a low-spin 6-coordinate ferric heme to a high-spin 5-coordinate species with loss of the thiolate ligand. Furthermore, addition of $HgCl_2$ to the ferric enzyme leads to slow conversion of the low-spin heme EPR signal to a high-spin signal (Figure 3). This parallels the changes observed by UV−visible absorption spectroscopy (Figure 1) and is consistent with loss of the thiolate ligand on exposure to $HgCl_2$.

The EPR spectrum of both full-length and truncated cystathionine β-synthase as isolated provides further evidence for thiolate coordination. The rhombic EPR signal (Figure 2) has g values that are similar to those of proteins and model heme complexes (*35*−*39*) with imidazole and thiolate ligands (Table 1). The narrow spacing between the g_z and g_x lines is typical of thiolate ligation (*39*). This is in contrast to the widespread g values in ferric cytochrome *c* (typically ranging from $g_{max} = 3.3$ to $g_{min} = 1.2$) where the axial heme ligands are imidazole and methionine (*40*−*42*). The EPR signal in human cystathionine β-synthase is insensitive to pH changes in the range of 6−9. This is in contrast to the rat H450 protein that displays two sets of closely spaced EPR signals [2.5, 2.31, 1.87 (acid form) and 2.4, 2.28, 1.91 (alkaline form)] that interconvert with a pK_a of ∼7 (*30*). The g values for the rat H450 protein and of human cystathionine β-synthase are similar to those of model heme complexes containing thiolate as a fifth ligand and an oxygen-, neutral sulfur-, or a nitrogen-donating group as the sixth ligand. Thus, the sixth ligand cannot be assigned on the basis of the characterization of the EPR spectrum alone. It should be noted, however, that the crystal field parameters determined for H450 (*30*) exclude an imidazole/methionine ligand pair and are consistent with an imidazole/thiolate ligand pair based on the low-spin heme correlation diagrams (*43*, *44*).

The MCD spectrum of the rat H450 protein also supports the assignment of a thiolate ligand in the ferric and ferrous states (*31*). However, a distinction between histidine versus methionine as the trans axial ligand to thiolate could not be made on the basis of the MCD data since the ferrous H450 spectrum was similar to those of the *N*-phenylimidazole and dimethyl sulfide complexes of ferrous P450-CAM, where the fifth ligand is a thiolate and the sixth is either an imidazole or a thioether (*31*).

Assignment of an Imidazole Ligand. The electronic absorption and EPR spectroscopic data reported here on human cystathionine β-synthase together with the MCD data on rat H450 provide strong evidence for the presence of a thiolate ligand but do not permit unequivocal distinction between histidine and methionine as the sixth heme ligand. The EXAFS results reveal that iron in ferric cystathionine β-synthase is 6-coordinate and is most consistent with ligation by 1 high-Z scatterer and 5 low-Z scatterers (Table 2). By arguing against coordination by two sulfurs (e.g., methionine and cysteine), the EXAFS, together with the EPR and MCD results, strongly suggests that cystathionine β-synthase contains an iron porphyrin that is axially coordinated to one histidine imidazole and one cysteine thiolate.

Conclusions. The spectroscopic properties of the human cystathionine β-synthase described in this study in combination with the MCD spectroscopic characterization of the rat enzyme, H450, support assignment of the axial ligands to the ferric heme as thiolate and imidazole. This combination of ligands is seen in another heme protein, CooA, which is a bacterial carbon monooxide sensor (*45*, *46*). Binding of carbon monooxide to the ferrous form of the protein elicits a conformational change that allows it to bind to DNA and function as a transcriptional regulator (*47*). Like CooA, cystathionine β-synthase binds carbon monooxide with high affinity, which is accompanied by loss of enzyme activity (*11*). However, CooA and cystathionine β-synthase do not share any obvious sequence homology, and the functional significance, if any, of the similar heme environments in the two proteins is unknown.

SUPPORTING INFORMATION AVAILABLE

Plots showing raw EXAFS data and best fits to these data using the parameters in Table 2. This material is available free of charge via the Internet at http://pubs.acs.org.

REFERENCES

1. Refsum, H., Ueland, P. M., Nygard, O., and Vollset, S. E. (1998) *Annu. Rev. Med. 49*, 31−62.
2. Mills, J. L., McPartlin, J. M., Kirke, P. N., Lee, Y. J., Conle, M. R., and Weir, D. G. (1995) *Lancet 345*, 149−151.
3. Steegers-Theunissen, R. P., Boers, G. H., Trijbels, F. J., and Eskes, T. K. (1991) *N. Engl. J. Med. 324*, 199−200.
4. Clarke, R., Smith, A. D., Jobst, K. A., Refsum, H., Sutton, L., and Ueland, P. M. (1998) *Arch. Neruol. 55*, 1449−1455.
5. Miller, J. W. (1999) *Nutr. Rev. 57*, 126−129.
6. Kang, S. S., Wong, P. W., and Malinow, M. R. (1992) *Annu. Rev. Nutr. 12*, 279−298.
7. Mudd, S. H., Levy, H. L., and Skovby, F. (1995) in *The Metabolic and Molecular Basis of Inherited Diseases* (Scriver, C. R., Beaudet, A. L., Sly, W. S., and Valle, D., Eds.) pp 1279−1328, McGraw-Hill, New York.
8. Borcsok, E., and Abeles, R. H. (1982) *Arch. Biochem. Biophys. 213*, 695−707.
9. Kery, V., Bukovska, G., and Kraus, J. P. (1994) *J. Biol. Chem. 269*, 25283−25288.
10. Finkelstein, J. D., Kyle, W. E., Martin, J. J., and Pick, A.-M. (1975) *Biochem. Biophys. Res. Commun. 66*, 81−87.
11. Taoka, S., West, M., and Banerjee, R. (1999) *Biochemistry 38*, 2738−2744.
12. Taoka, S., Widjaja, L., and Banerjee, R. (1999) *Biochemistry 38*, 13155−13161.
13. Kery, V., Poneleit, L., and Kraus, J. (1998) *Arch. Biochem. Biophys. 355*, 222−232.
14. Shan, X., and Kruger, W. D. (1998) *Nat. Genet. 19*, 91−93.
15. Kabil, O., and Banerjee, R. (1999) *J. Biol. Chem. 274*, 31256−31260.
16. Taoka, S., Ohja, S., Shan, X., Kruger, W. D., and Banerjee, R. (1998) *J. Biol. Chem. 273*, 25179−25184.
17. McMaster, W. H., Del Grande, N. K., Mallett, J. H., and Hubbell, J. H. (1969) U.S. Department of Commerce Report No. UCRL-50174-SEC 2-R1.
18. Teo, B. K. (1986) in *EXAFS: Basic Principles and Data Analysis*, Springer-Verlag, New York.
19. Rehr, J. J., Mustre, d. L. J., Zabinsky, S. I., and Albers, R. C. (1991) *J. Am. Chem. Soc. 113*, 5135−5140.
20. Roe, A. L., Schneider, D. J., Mayer, R. J., Pyrz, J. W., Widom, J., and Que, L. J. (1984) *J. Am. Chem. Soc. 106*, 1676.

21. Penner-Hahn, J. E., and Hodgson, K. O. (1989) in *Iron Porphyrins* (Lever, A. B. P., and Gray, H. B., Eds.) Part III, pp 235−304, VCH Publishers, Inc., New York.
22. Riggs-Gelasco, P. J., Stemmler, T. L., and Penner-Hahn, J. E. (1995) *Coord. Chem. Rev. 144*, 245−286.
23. Clark-Baldwin, K., Tierney, D. L., Govindaswamy, N., Gruff, E. S., Kim, C., Berg, J., Koch, S. A., and Penner-Hahn, J. E. (1998) *J. Am. Chem. Soc. 120*, 8403−8409.
24. Thorp, H. H. (1992) *Inorg. Chem. 31*, 1585−1588.
25. Liu, W. T., and Thorp, H. H. (1993) *Inorg. Chem. 32*, 4102−4105.
26. Kraus, J., Packman, S., Fowler, B., and Rosenberg, L. E. (1978) *J. Biol. Chem. 253*, 6523−6528.
27. Kraus, J. P., and Rosenberg, L. E. (1983) *Arch. Biochem. Biophys. 222*, 44−52.
28. Kim, I. C., and Deal, W. C. J. (1976) *Biochemistry 2*, 4925−4930.
29. Hasegawa, T., Sadano, H., and Omura, T. (1984) *J. Biochem. 96*, 265−268.
30. Omura, T., Sadano, H., Hasegawa, T., Yoshida, Y., and Kominami, S. (1984) *J. Biochem. 96*, 1491−1500.
31. Svastits, E. W., Alberta, J. A., Kim, I.-C., and Dawson, J. H. (1989) *Biochem. Biophys. Res. Commun. 165*, 1170−1176.
32. Ishihara, S., Morohashi, K.-i., Sadano, H., Kawabata, S.-i., Gotoh, O., and Omura, T. (1990) *J. Biochem. 108*, 899−902.
33. Cheesman, M. R., Thomson, A. J., Greenwood, C., Moore, G. R., and Kadir, F. (1990) *Nature 346*, 771−773.
34. Dawson, J. H., and Sono, M. (1987) *Chem. Rev. 87*, 1255−1276.
35. Chevion, M., Peisach, J., and Blumberg, W. E. (1977) *J. Biol. Chem. 252*, 3637−3645.
36. Kraus, D. W., Wittenberg, J. B., Jing-Fen, L., and Peisach, J. (1990) *J. Biol. Chem. 265*, 16054−16059.
37. Aono, S., Ohkubo, K., Matsuo, T., and Nakajima, H. (1998) *J. Biol. Chem. 273*, 25757−25764.
38. Reynolds, M. F., Shelver, D., Kerby, R. L., Parks, R. B., Roberts, G. P., and Burstyn, J. N. (1998) *J. Am. Chem. Soc. 120*, 9080−9081.
39. Dawson, J. H., Andersson, L. A., and Sono, M. (1982) *J. Biol. Chem. 257*, 3606−3617.
40. Salmeen, I., and Palmer, G. (1968) *J. Chem. Phys. 48*, 2049−2052.
41. Gadsby, P. M., Hartshorn, R. T., Moura, J. J., Sinclair-Day, J. D., Sykes, A. G., and Thomson, A. J. (1989) *Biochim. Biophys. Acta 994*, 37−46.
42. Arciero, D. M., Peng, Q., Peterson, J., and Hooper, A. B. (1994) *FEBS Lett. 342*, 217−220.
43. Blumberg, W. E., and Peisach, J. (1971) *Probes of Structure and Function of Macromolecules and Membranes*, pp 215−229, Academic Press, New York.
44. Palmer, G. (1983) in *Electron Paramagnetic Resonance of Hemoproteins* (Lever, A. B. P., and Gray, H. B., Eds.) VCH Publishers, New York.
45. Dhawan, I. K., Shelver, D., Thorsteinsson, M. V., Roberts, G. P., and Johnson, M. K. (1999) *Biochemistry 38*, 12805−12813.
46. Shelver, D., Thorsteinsson, M. V., Kerby, R. L., Chung, S. Y., Roberts, G. P., Reynolds, M. F., Parks, R. B., and Burstyn, J. N. (1999) *Biochemistry 38*, 2669−2678.
47. Shelver, D., Kerby, R. L., He, Y., and Roberts, G. P. (1997) *Proc. Natl. Acad. Sci. U.S.A. 94*, 11216−11220.

BI000831H